Black Sea Journal of Engineering and Science
doi: 10.34248/bsengineering.1852119

Open Access Journal
e-ISSN: 2619 – 8991

Research Article
Volume 9 - Issue 2: 914-921 / March 2026

STRUCTURAL EVALUATION OF AN AIRCRAFT WING WITH A REPAIRED FRONT SPAR

Gurkan ORTAMEVZI[1]*

[1]*Alanya Alaaddin Keykubat University, Faculty of Gazipasa Aerospace Sciences, Department of Aviation Management, 07900, Antalya, Türkiye*

Abstract: This article hypothesizes that the leading spar of an experimental aircraft wing is damaged, and that this damage will be repaired using different variations. The effect of these repairs on the wing's strength is investigated. Aircraft accidents and incidents caused by damage or cracks in the leading spar served as the basis for this study. 3D models of all repair variations were created, and mathematical mesh models were developed to examine the strength parameters generated using the finite element method. The von-Mises stress, shear stress, safety factor, and wingtip deformation in the repaired area of the leading spar were compared according to the repair variations to evaluate the wing's strength. Furthermore, the strength condition was also evaluated based on the damaged spar sector. During the evaluations, the strength parameters were examined using an undamaged wing as a reference.

Keywords: Front spar, Spar repair, Finite element method, Wing strength, von-Mises stress, Shear stress

***Corresponding author:** Alanya Alaaddin Keykubat University, Faculty of Gazipasa Aerospace Sciences, Department of Aviation Management, 07900, Antalya, Türkiye
E mail: gurkan.ortamevzi@alanya.edu.tr (G. ORTAMEVZI)
Gurkan ORTAMEVZI https://orcid.org/0000-0002-6380-2575

Received: December 30, 2025
Accepted: March 01, 2026
Published: March 15, 2026

Cite as: Ortamevzi, G. (2026). Structural evaluation of an aircraft wing with a repaired front spar. *Black Sea Journal of Engineering and Science*, *9*(2), 914-921.

1. Introduction

Wings are the most important components in aircraft, generating lift and carrying the entire weight of the aircraft during flight. The supporting columns in the structure of aircraft wings are called spars. Wide-chord wings usually have three spars. These three spars are positioned at the front, rear, and possibly at the center of gravity. In addition to supporting the weight of the aircraft during flight, the spars also support the weight of the fuel and the wing itself when parked or taxiing. Furthermore, since flight control surfaces are mounted on the spars, they withstand loads from these surfaces. Impact loads generated during landing are also indirectly transmitted to the spars. Aerodynamic loads on the wings of an aircraft exposed to gusts of rain during flight are also withstood by the spars. The air and ground loads to which the spars are subjected vary greatly in size and application, creating very different tensile, compressive, and shear stresses, and combinations of these stresses. Over time, these stresses can cause fatigue-related cracks and damage in the spars, or cracks and damage can occur suddenly when they reach the yield or fracture stress level. Apart from these, damage caused by external factors unrelated to exploration activities (collisions, impacts during maintenance or assembly, etc.) can cause the integrity of the spars to be compromised. This compromise directly affects flight safety. Detecting these cracks and damages during inspection is vital, and repairing the damaged spar correctly is crucial. Many accidents have been reported due to front spar damage. According to the National Transportation Safety Board (NTSB) report on accident FTW99FA123, a critical crack in the right wing front spar of a Cessna 402C aircraft, which had developed over time, resulted in the wing breaking off, causing the aircraft to crash and resulting in fatalities (National Transportation Safety Board, 1999). According to the NTSB's report on accident number WPR21FA266, a fatigue crack formed in the left wing front spar of a Beechcraft C90 aircraft due to heavy load usage. This resulted in the spar losing its integrity, followed by the wing breaking off, leading to a fatal accident. The report states that the crack in the front spar had been detected previously, but the aircraft manufacturer's recommendation to replace the entire spar was ignored; instead, it was only repaired, and the aircraft continued to be used. (National Transportation Safety Board, 2023). Besides numerous fatal accidents caused by similar front spar damage, there are also many incident cases where damage was previously identified (National Transportation Safety Board, 2005; European Aviation Safety Agency, 2008; National Transportation Safety Board, 2018).

This study analyzes the strength of a three-spar aircraft wing with a NACA-4412 profile, specifically focusing on the repaired front spar, under critical loading. 3D models of the damaged and repaired front spar were created, followed by a mathematical mesh model. The wing was then subjected to loading simulations using the Finite

Element Method (FEM). The repair process was modeled with varying numbers of rivets, and multiple scenarios were simulated by loading from different regions. Following the simulations, the equivalent stress, shear stress, total deformation, and safety factor strength parameters were compared, particularly focusing on the repaired region. This study focuses solely on front spar damage modeling but is also a guide for researchers who will be modeling damage to other critical components.

2. Materials and Methods

2.1. Theory

The spars on aircraft wings act as supporting columns and are therefore subjected to significant stress. While an undamaged spar carries a load for example, when the wings support the aircraft, the upper surface of the spar is subjected to compressive stress, and the lower surface to tensile stress. Of course, the stringers and wing coverings that bear the stresses of the spars in the wing structure create a complex system for analyzing the spar's stress state. Furthermore, for a spar repaired using rivets, the rivet contact areas will transfer tensile and compressive stresses to the rivets as shear stresses. When a repaired spar is subjected to complex stresses consisting of tensile, compressive, shear stresses, and combinations thereof, calculating its strength using classical methods becomes very challenging (Budynas et al., 2011). In this study, since numerous repair variations were evaluated, determining the strength parameters using the finite element method was deemed appropriate (Langrand et al., 2001; Keçelioğlu, 2008; Kondo et al., 2021).

2.2. 3D Damaged and Repaired Wing Model and Mathematical Mesh Model

The wing section of an experimental aircraft with a NACA-4412 airfoil profile, with a wingspan of one meter, is an example of this study. This wing has three spars. It was assumed that there was damage in the second sector of the front spar, and the damaged portion of the spar was removed and patched with a similar spar piece. In creating the 3D model of this patched wing, the rivets, which were installed in different numbers and positions during the repair, were modeled. To analyze whether the repair preserved the integrity of the spars, 3D models of several repair variations were created. Furthermore, to investigate the effect of the proximity of the damage to the wing root on wing strength, an analog of a repair version was applied to the first spar sector and a 3D model was created. Each repair variation was named to be discussed in other parts of the study. The 3D models of the damaged and repaired wing are shown in Figure 1, and the repair variations are shown with their names in Table 1.

Mathematical mesh models were created for all 3D repair models to calculate the wing's strength properties using the finite element method. A higher mesh density was used in the repair area to increase computational accuracy in that region. The 5*2+4 model shown in Table 1 uses 461374 nodes and 224373 elements. The mathematical mesh model of the 5*2+4 3D model is shown in Figure 2. Similar mathematical mesh models with similar mesh structures and numbers were also created for the other 3D models.

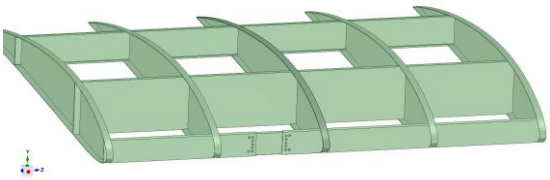

Figure 1. 3D model of damaged and repaired wing.

Table 1. Repair variations and names of repair variations*

3D model of repair variations	Name of repair variations
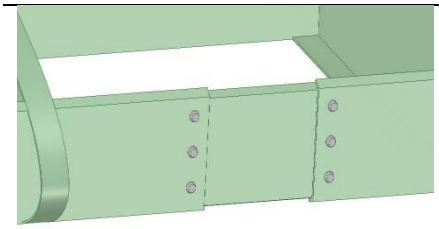	3*2
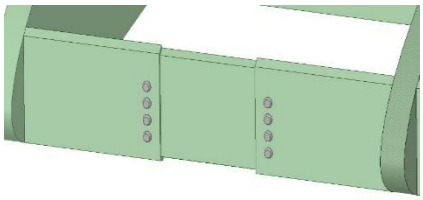	4*2
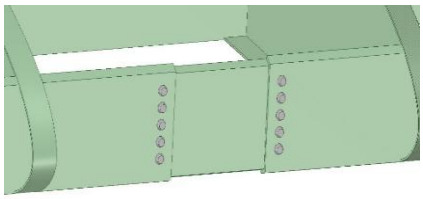	5*2
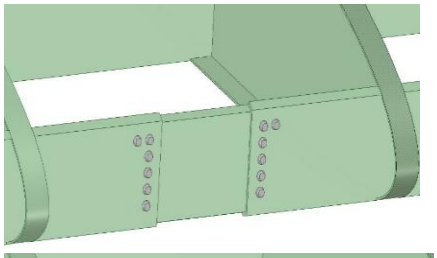	5*2 + 2 upside
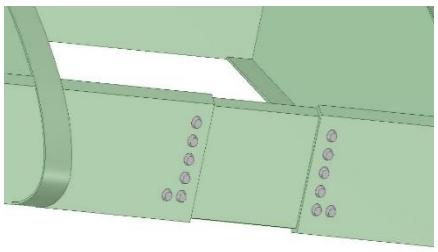	5*2 + 2 downside

*Repair model names are related to the number and sequence of rivets used in the repair process.

Table 1. Repair variations and names of repair variations* (continued)

3D model of repair variations	Name of repair variations
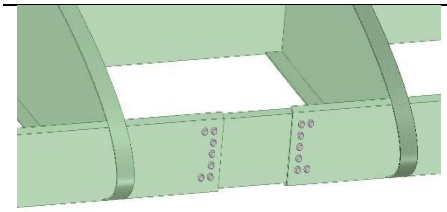	5*2 + 4
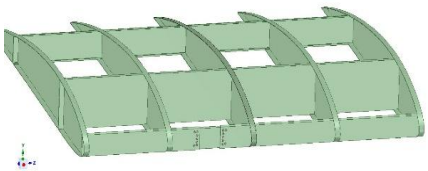	2nd sector repair
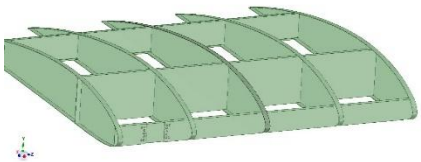	1st sector repair
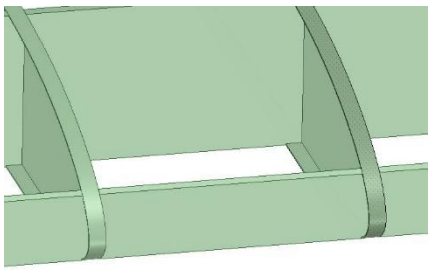	No damage

*Repair model names are related to the number and sequence of rivets used in the repair process.

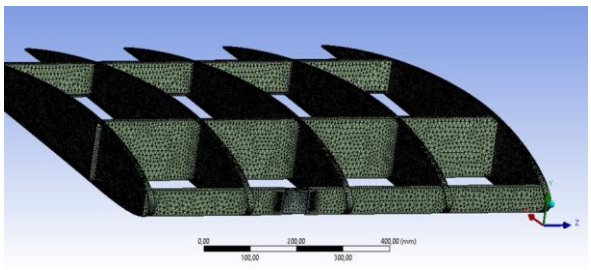

Figure 2. Mathematical mesh model of 5*2+4 damaged and repaired wing.

2.3. Simulation of Wing under Forces

In Figure 3, the experimentally repaired left wing spars were simulated as if they were fixed to the aircraft at their roots, while a force of 2000N was applied from the wingtip, between the main and front spars, in the direction of lift. This simulation was applied to all repair variations with the same location and magnitude of the force. Shifting the center of gravity towards the nose will negatively affect wing strength. The limiting line in the upper left of the aircraft's center of gravity envelopes is the limiting line for wing strength (Kaya, 2022). Since the aircraft under consideration is a fixed-wing unmanned aerial vehicle (UAV), the magnitude and location of the applied load were determined according to the aircraft's weight and basic flight characteristics. In level flight, the total lift force is equal to the aircraft's weight, while during maneuvers it varies according to load factors. For a representative UAV's maximum takeoff weight, a highly positive maneuver load factor can result in a total lift force approximately three times greater. Since this model represents a single wing, this load is distributed between the two wings, meaning each wing carries approximately half of the load. A force of 2000N applied to the wingtip represents a realistic loading condition for the UAV under consideration, corresponding to a highly maneuverable load. The repaired left wing is assumed to have a lift force of 1000 N. The load factor here is assumed to be n ≈ 2 and gust loads have been considered (Majka, 2013; Zheng et al., 2025). However, critical potential load conditions were also analyzed for 5*2 + 4 repair variations. Here, negative load factors, torsional loading, and wind-induced loads were considered in the simulation.

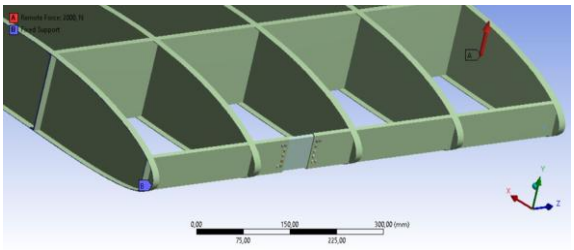

Figure 3. Simulation of forces and fixed support.

3. Results and Discussion

Aluminum 2024, a material frequently used in aircraft wing production, is assumed to be used in the production of this experimental wing. Aluminum 2024 has a yield stress of σy = 325 MPa (Hirsch et al., 2008; Pippig et al., 2017). According to the simulation performed on an undamaged wing, the stress reached its maximum at the lower root portion of the main spar, observed to be 264.8 MPa with a safety factor of 1.23. However, when repair was performed on the first and second sectors of the front spar, the maximum stress shifted to the front spar repair region in all cases. Figure 4 graphs the maximum von-Mises stress and maximum shear stress values in the marked region according to the name of repair variations. The marked region has the greatest stresses in the entire wing construction.

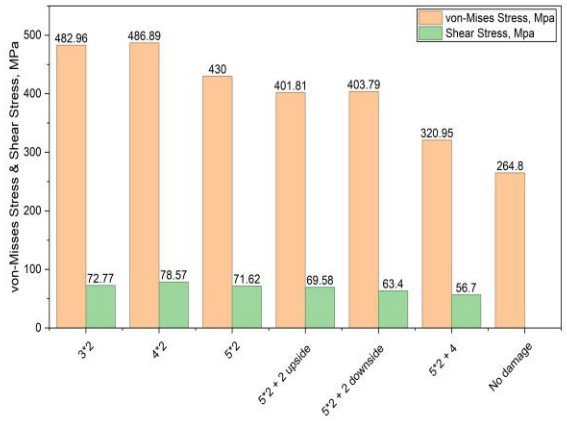

Figure 4. Maximum von-Mises stress and maximum shear stress according to name of repair variations.

The 5*2+4 repair model was applied to both the first and second spar sectors of the same wing to create a simulation. The maximum von-Mises stress and maximum shear stress values in the marked regions of these simulations are shown in Figure 5 for comparison with the undamaged wing.

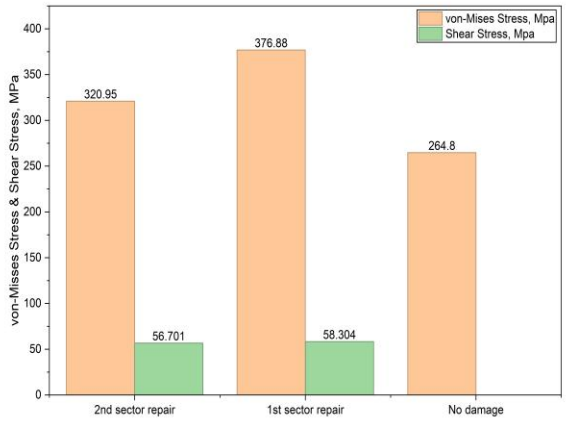

Figure 5. Maximum von-Mises stress and maximum shear stress according to the spar sector of the 5*2+4 repair model.

The deformation occurring at the free end of the wing was compared for both the name of repair variations and the spar sector of the 5*2+4 repair model. Increased wingtip deformation reduces the lift force in the wing where the deformation occurs (Zheng et al., 2025). Safety factor values have also been determined for aluminum 2024 material. The safety factor is a design criterion, and if it is below 1, there is a high probability of permanent deformation in the wing structural elements. These comparative graphs are shown in Figures 6 and 7.
Stress distributions for all repair variations are shown in Table 2.

Valuable Validation of Finite Element Method Results Based on Quantitative Comparison with Literature

The results of this study were examined by quantitatively comparing them with studies in the literature based on the finite element method that address riveted aircraft connections and wing structural components. One study analyzed riveted aircraft structural connections subjected to tensile loads of 2 kN. It reported that this load created a maximum rivet shear stress of 80 MPa, corresponding to a rivet body yield strength of approximately 180 MPa (Kondo et al., 2021). This value corresponds to a stress-yield ratio of approximately 0.44. The results emphasize that the applied load was carried by the top and bottom rivets, and that increasing the number of rivets in the same row did not significantly affect the stress values at the top and bottom rivets. In this study, a wingtip static load of 2000 N created a maximum von-Misses stress of 320.95 MPa in the 5*2+4 repair model located in the second spar sector. This value represents a tensile yield ratio of 0.99 when compared to the yield strength of aluminum 2024, which is 325 MPa. Although the stress value of 320.95 MPa is higher than the shear stress of 80 MPa reported by Kondo et al., the difference is related to the design configuration and is mechanically consistent with differences in structural configuration. However, the higher stress magnitude in this study is due to the large bending moments acting at the wing root, compared to the local loading configuration in the joint region in Kondo et al.'s study. The load transfer is also mathematically consistent. In this study, in single-row rivet variations, the greatest stresses occur in the upper rivet region near the wing root, while the addition of a second row of rivets shifts the location of the weak region to the lowest rivet region. However, increasing the number of rivets in the same row does not significantly reduce the maximum stress at the end rivets. This directly coincides with the results reported by Kondo et al. Here, stress concentration remains dominant in the upper and lower rivets, even after increasing the number of rivets.

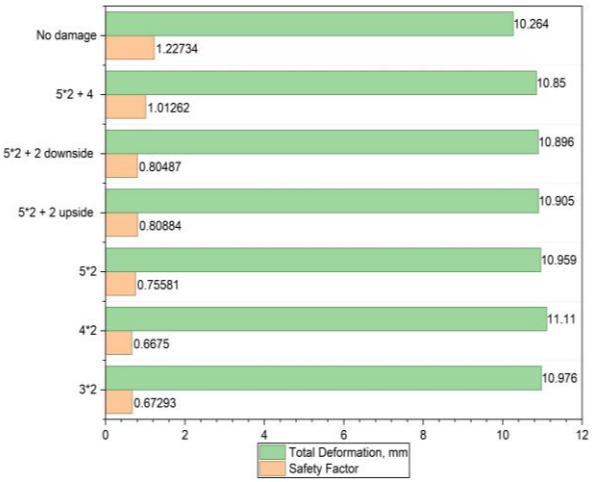

Figure 6. Total deformation and safety factor according to name of repair variations.

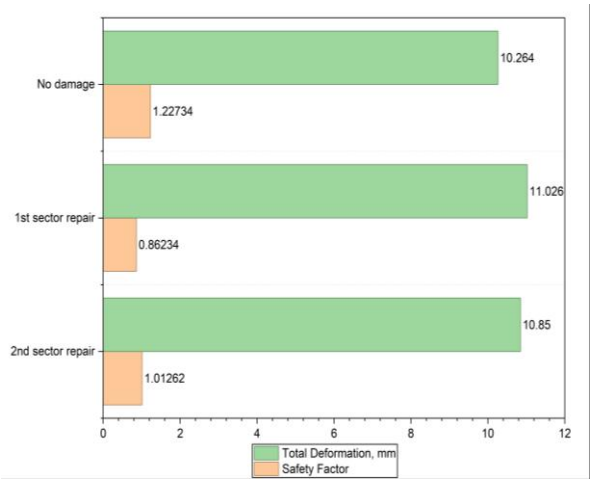

Figure 7. Total deformation and safety factor according to the spar sector of the 5*2+4 repair model

Table 2. Stress distribution according to repair variations

Stress Distribution	Name of repair variations
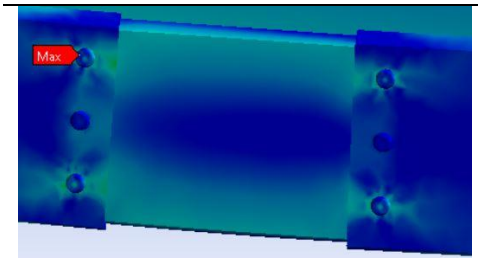	3*2
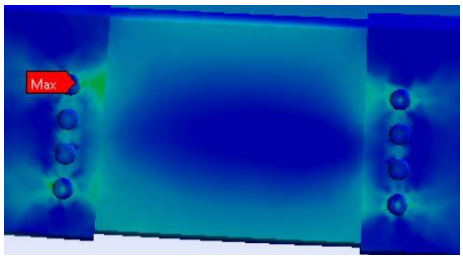	4*2
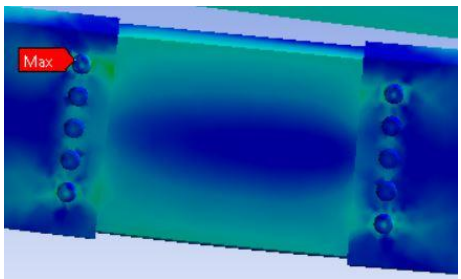	5*2
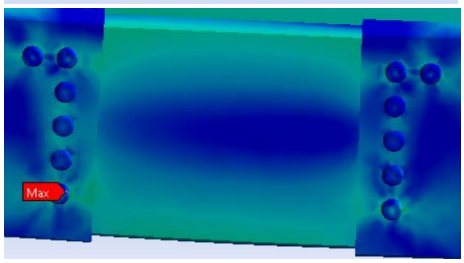	5*2 + 2 upside

Table 2. Stress distribution according to repair variations (continued)

Stress Distribution	Name of repair variations
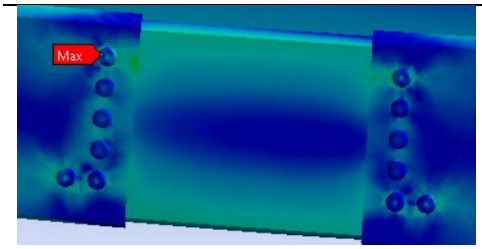	5*2 + 2 downside
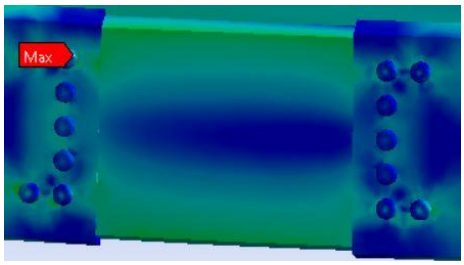	5*2 + 4
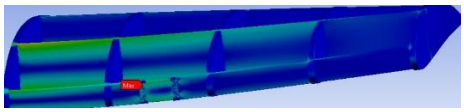	2nd sector repair
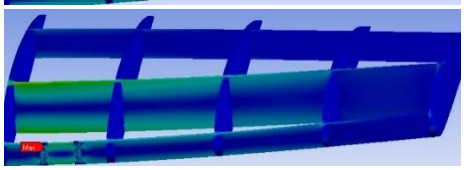	1st sector repair
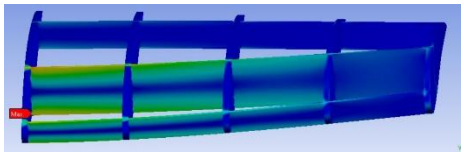	No damage

In their studies, which generated results using finite element method analysis, they examined aircraft wing spars subjected to static bending loads (Saravanan et al., 2018). Wing loading simulation showed that the von-Misses stress value at the wing root, where bending moments are greatest, can approach the material yield limit. Similar results were observed in this study, and they are consistent with the results of Saravanan et al. (2018). The decrease in stress as the repair area moves away from the wing root was observed in the same way. However, the increased wingtip deformation in the repaired front spar variations in this study is due to the deterioration of the rigidity of the structural elements in the undamaged structure, which is mechanically consistent and coincides with the elastic redistribution behavior observed in the finite element method analyses. Table 3 compares this study with the two similar studies mentioned.

Table 3. Stress distribution according to repair variations

Parameters	Kondo et al. (2021)	Saravanan et al. (2018)	Present Study
Structural configuration	Riveted aircraft joint specimen	Wing-like beam structure	Riveted repaired front spar
Analysis method	Finite Element Method	Finite Element Method	Finite Element Method
Applied load magnitude	≈ 2 kN	Static bending loads	2000 N
Load equivalence	Same order as present study	Root-dominated bending	Equivalent load level (2 kN)
Material	Aircraft-grade aluminum (rivet)	Aluminum alloys	Aluminum 2024
Stress output type	Rivet shear stress	von Mises stress	von Mises stress
Maximum stress value	≈ 80 MPa (Shear stress)	Near-yield stresses reported	320.95 MPa
Material yield strength	≈ 180 MPa	Aluminum yield limit	325 MPa
Stress-to-yield ratio	≈ 0.44	Approaching unity in critical regions	≈ 0.99
Location of maximum stress	Upper and lower rivets	Root region	Root / rivet-adjacent region
Effect of increasing fastener number	Limited reduction in peak stress	Local stress governed by global bending	Limited reduction in peak stress
Effect of structural location	Higher stress near root	Higher stress near root	Higher stress near root
Structural regime	Linear elastic	Linear elastic	Linear elastic

What distinguishes this study from others is that while other studies investigated riveted connections and wing spars separately, this study investigated wing spars repaired with rivets. In other words, it is a combination of other studies.

As seen from the results, the repair variation with the lowest von-Misses stress magnitude is the 5*2+4 repair variation. However, for the 5*2+4 repair variation performed in the second spar sector, the analyses were repeated considering other predicted aerodynamic loads during the flight of the unmanned aerial vehicle. The aim here is to predict the behavior of the front spar under other loads that the UAV may encounter during flight. These other loads include aerodynamic torsional moment (torsion), gust load, and negative maneuvering situations (push-over, sudden descent).

In actual flight, while the wing generates positive lift, it operates under both bending and torsion forces. If the location of the 2000 N load applied from the wingtip, i.e., the aerodynamic center does not coincide with the shear center, a torsion moment occurs. In this simulation, it was assumed that there is a distance of 0.1 m between the aerodynamic center and the shear center, and that the torsion moment occurs according to this distance and is applied to the wing together with the bending force. The magnitude of the torsion moment can be calculated using equation 1 (Voß, 2020).

$$T = L \cdot e \quad (1)$$

Here, T is the torsion moment, L is the total lift, and e is the distance between the aerodynamic center and the shear center.

In this case, the torsion moment is 200 Nm. The model created for analysis, which simulates positive lift and torsion moment, is shown in Figure 8.

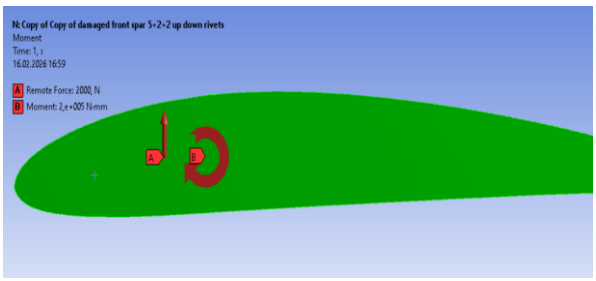

Figure 8. A simulation in which positive lift force and torsional moment are applied simultaneously

Additionally, the scenario where negative lift force could occur was simulated and the analyses were repeated. For small UAVs, n ≈ −1 was assumed, and a negative lift force of 1000 N was applied to the wingtip (Majka, 2013). The critical von-Mises stress value and distribution in the front spar repair region are shown in Figure 9 for simultaneously applied positive lift force and torsion moment, and in Figure 10 for negative lift force.

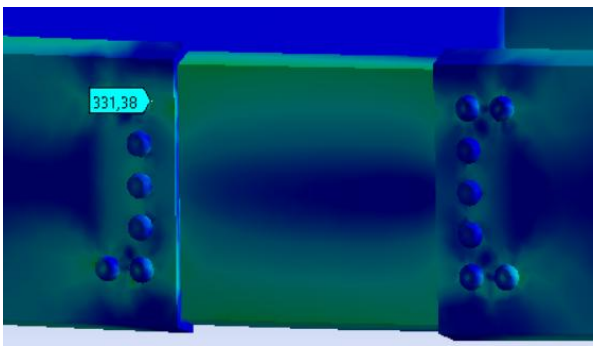

Figure 9. Von-Misses stress value and distribution for simultaneously applied positive lift force and torsional moment (The maximum stress is 331.38 MPa.).

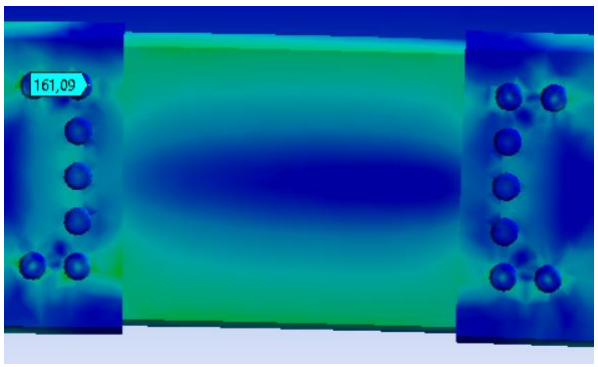

Figure 10. Von-Misses stress value and distribution for applied negative lift force (The maximum stress is 161.09 MPa.).

4. Conclusion

When a single row of rivets is used in the front spar repair, the highest stress values are observed in the uppermost rivet region at the root end. If a second row of rivets is added next to this rivet, the highest stress shifts to the lowest rivet. In other words, a very large portion of the stress load is borne by the top and bottom rivets. Increasing the number of rivets in the same row does not significantly reduce the stress experienced by the top and bottom rivets.

In the 5*2+4 repair model in the second spar sector, the von-Mises stress magnitude was determined to be 320.95. This did not exceed the yield stress value of 325 MPa for aluminum 2024 material. However, since it did not reach the 1.23 safety factor value of the undamaged wing, the maximum allowed take-off weight, landing weight, and zero fuel weight values should be reduced while the aircraft is in use. Furthermore, narrowing the aircraft's center of gravity envelope from the nose will provide safer flight during deployment.

When comparing 5*2+4 repair models according to the first and second spar sectors, the repair area being closer to the wing root causes greater stress. While this repair model is observed to not exceed the yield stress value in the second spar sector, it is observed to exceed the yield stress value in the first spar sector with a safety factor of 0.86. In other words, the stress value decreases as the repair area moves further away from the wing root.

In any case, a wing with a repaired front spar will have increased wingtip deformation compared to an undamaged wing. This is expected to asymmetrically alter the lift force and disrupt the roll motion balance. If the aircraft has a roll trim tab, the roll trim tab limits must be carefully calculated to tolerate the asymmetric lift force caused by this deformation. This is especially critical in aircraft with large wingspans. Furthermore, an aircraft flying with continuously angled ailerons will experience increased drag and fuel consumption.

In an aircraft with a repaired front spar, under positive lift and gust loads, even if the stresses in the repair area are within the yield limits of the material, there is a high probability that they will exceed the yield limit due to other aerodynamic loads. In particular, the torsional moment generated in the wing amplifies the stress, pushing it into the critical region and exceeding the yield limit of the material. If an aircraft with a repaired front spar is in use, it should be loaded so that its center of gravity is close to the aerodynamic center of the wing. This will reduce the potential torsional moment.

In an aircraft with a repaired front spar, under negative lift ($n \approx -1$), the maximum stress is 161.09 MPa, with an approximate safety factor of 2.

Author Contributions

The percentages of the author' contributions are presented below. The author reviewed and approved the final version of the manuscript.

	H.A.
C	100
D	100
S	100
DCP	100
DAI	100
L	100
W	100
CR	100
SR	100
PM	100
FA	100

C= concept, D= design, S= supervision, DCP= data collection and/or processing, DAI= data analysis and/or interpretation, L= literature search, W= writing, CR= critical review, SR= submission and revision, PM= project management, FA= funding acquisition.

Conflict of Interest

The author declares no conflict of interest. The funders had no role in the design of the study; in the collection, analysis, or interpretation of data; in the writing of the manuscript, or in the decision to publish the results.

Ethical Consideration

This study did not involve human participants or animals and therefore did not require ethics committee approval.

References

Budynas, R. G., & Nisbett, J. K. (2011). *Shigley's mechanical engineering design* (9th ed.). McGraw-Hill.

European Aviation Safety Agency. (2008). *Airworthiness directive: CF-2007-31 – DHC-6 Twin Otter wing front spar adapter cracks* (Issue CF-2007-31). https://ad.easa.europa.eu/ad/CF-2007-31

Hirsch, J., Skrotzki, B., & Gottstein, G. (Eds.). (2008). *Aluminium alloys: The physical and mechanical properties* (Vol. 1). John Wiley & Sons.

Kaya, İ. (2022). *The effect of center of gravity and shear center locations on flutter behavior of wings* (Unpublished thesis, University of Turkish Aeronautical Association).

https://doi.org/10.13140/RG.2.2.36231.27048

Keçelioğlu, G. (2008). *Stress and fracture analysis of riveted joints* (Master's thesis, Middle East Technical University). OpenMETU. https://open.metu.edu.tr/handle/11511/18070

Kondo, A., Kasahara, T., & Kanda, A. (2021). A simplified finite element model of riveted joints for structural analyses with consideration of nonlinear load-transfer characteristics. *Aerospace, 8*(7), 196. https://doi.org/10.3390/aerospace8070196

Langrand, B., Deletombe, E., Markiewicz, E., & Drazetic, P. (2001). Riveted joint modeling for numerical analysis of airframe crashworthiness. *Finite Elements in Analysis and Design, 38*(1), 21–44. https://doi.org/10.1016/S0168-874X(01)00050-6

Majka, A. (2013). Flight loads of mini UAV. *Solid State Phenomena*, *198*, 194-199. https://doi.org/10.4028/www.scientific.net/SSP.198.194

National Transportation Safety Board. (1999). *Aviation investigation final report: Accident number FTW99FA123—Cessna 402C, N819BW, Goldsby, Oklahoma* (Report No. FTW99FA123). https://data.ntsb.gov/carol-repgen/api/Aviation/ReportMain/GenerateNewestReport/46183/pdf

National Transportation Safety Board. (2005). *Aviation investigation final report: Incident number SEA05IA115—Piper PA-46-350P wing lower spar cap crack found during inspection* (Report No. SEA05IA115). https://data.ntsb.gov/carol-repgen/api/Aviation/ReportMain/GenerateNewestReport/61685/pdf

National Transportation Safety Board. (2018). *Materials laboratory factual report: ERA18FA120—Piper PA-28R wing spar lower cap fatigue cracking* (Report No. ERA18FA120). https://data.ntsb.gov/Docket/Document/docBLOB?FileExtension=pdf&FileName=ERA18FA120+Structures+Factual-Rel.pdf&ID=7869710

National Transportation Safety Board. (2023, August 23). *Aviation investigation final report: Accident number WPR21FA266—Beech C90, N3688P, Wikieup, Arizona* (Report No. WPR21FA266). https://data.ntsb.gov/carol-repgen/api/Aviation/ReportMain/GenerateNewestReport/103452/pdf

Pippig, R., Schmidl, E., Steinert, P., Schubert, A., & Lampke, T. (2017). Experimental and numerical investigation of the residual yield strength of aluminium alloy EN AW-2024-T3 affected by artificially produced pitting corrosion. *IOP Conference Series: Materials Science and Engineering, 181*(1), 012023. https://doi.org/10.1088/1757-899X/181/1/012023

Saravanan, G., Johnson, A. A., & Pandiarajan, P. (2018). Finite element analysis of aircraft wing joint and fatigue life prediction under variable loading using MSC Patran and Nastran. *International Journal of Mechanical Engineering and Technology, 9*(11), 1111–1119. http://iaeme.com/Home/issue/IJMET?Volume=9&Issue=11

Voß, A. (2020). *Design and structural optimization of a flying wing of low aspect ratio based on flight loads* (Doctoral dissertation, Technische Universität Berlin).

Zheng, Y., Dai, Y., Huang, G., & Hu, Y. (2025). Gust response alleviation via wingtip bending freely with fluid-structure interaction approach based on dynamic modal rotation method. *Chinese Journal of Aeronautics*. Advance online publication. https://doi.org/10.1016/j.cja.2025.103851